

## Phased-array Antenna System for Electron Bernstein Wave Heating and Current Drive Experiments in QUEST

H. Idei 1), M. Sakaguchi 2), E.I. Kalinnikova 2), K. Nagata 2), A. Fukuyama 3), H. Zushi 1), K. Hanada 1), M. Ishiguro 2), H. Igami 4), S. Kubo 4), K. Nakamura 1), A. Fujisawa 1), M. Sakamoto 1), M. Hasegawa 1), Higashizono 1), S. Tashima 2), R. Ogata 2), H. Q. Liu 2), I. Goda 2), T. Ryokai 2), S. K. Sharma 2), M. Isobe 4), A. Ejiri 5) K. Nagaoka 4), M. Osakabe 4), A. Tsushima 6), H. Nakanishi 1), T. Morisaki, 4), N. Nishino 7), Y. Nakashima 8), H. Watanabe 1), K. Tokunaga 1), T. Tanabe 2), N. Yoshida 1), K.N. Sato 2), S. Kawasaki 1), H. Nakashima 1), A. Higashijima 1), Y. Takase 5), T. Maekawa 9), O. Mitarai 10) M. Kikuchi 11), K. Toi 4) and Y. Kishimoto 9)

- 1) Research Institute for Fusion Science, Kasuga, 816-8580, Japan
- 2) Interdisciplinary Grad. School of Eng. Sci., Kyushu Univ., Kasuga, 816-8580, Japan
- 3) Department of Nuclear Engineering, Kyoto Univ., Kyoto, 606-8501, Japan
- 4) National Institute for Fusion Science, Toki, 509-5292, Japan
- 5) Department of Complexity Sci. and Eng., Univ. of Tokyo, Kashiwa, 277-8561, Japan
- 6) Faculty of Engineering, Yokohama National Univ., Yokohama, 240-8501, Japan
- 7) Mechanical System Engineering, Hiroshima Univ., Hiroshima, 739-8527, Japan
- 8) Plasma Research Center, Tsukuba Univ., Tsukuba, 305-8577, Japan
- 9) Graduate School of Energy Science, Kyoto Univ., Kyoto, 606-8501, Japan
- 10) Inst. of Ind. Sci. and Tech. Research, Tokai Univ., Kumamoto, 862-8652, Japan
- 11) Japan Atomic Energy Agency, Naka, 311-0193, Japan

E-mail contact of main author: [idei@triam.kyushu-u.ac.jp](mailto:idei@triam.kyushu-u.ac.jp)

**Abstract** The phased-array antenna system for Electron Bernstein Wave Heating and Current Drive (EBWH/CD) experiments has been developed in the QUEST. The antenna was designed to excite a pure O-mode wave in the oblique injection for the EBWH/CD experiments, and was tested at a low power level. The measured two orthogonal fields were in excellent agreements with the fields evaluated by a developed Kirchhoff code. The heat load and thermal stress in CW 200 kW operation were analyzed with finite element codes. The phased array has been fast scanned [ $\sim 10^4$  degree/s] to control the incident polarization and angle to follow time evolutions of the plasma current and density. The RF startup and sustainment experiments were conducted using the developed antenna system. The plasma current ( $< \sim 15$  kA) with an aspect ratio of 1.5 was started up and sustained by only RF injection. The long pulse discharge of 10 kA was attained for 40 s with the 30 kW injection.

### 1. Introduction

The spherical tokamak (ST) has a capability to attain higher  $\beta$  than conventional tokamaks. The Q-shu university experiment with steady state spherical tokamak (QUEST) was proposed at Kyushu University, and the QUEST device has been constructed [1]. A final target of the project is the steady state operation with relatively high  $\beta$  ( $< 10\%$ ) in the ST configuration under controlled plasma wall interactions (PWI). For the steady state operation, the plasma current drive method should be established. Electron Bernstein wave heating and current drive (EBWH/CD) is one of attractive candidates of heating and current drive method to sustain the steady-state ST plasma. The EBWH experiments were demonstrated in high-density plasmas beyond the cutoff at the W-7AS stellarator [2], and then were conducted in many devices [3]. In the ST experiments, the plasma frequency may become larger than the electron cyclotron frequency in the operating density range due to the rather low magnetic field, and electron cyclotron waves cannot propagate into the plasma beyond the cutoff layers. In the EBWH/CD experiments, some mode conversions from the electron cyclotron (electromagnetic) wave to the electron Bernstein B- (electrostatic) wave are required. In the O-X-B mode conversion

experiments, the launching angle and elliptical polarization state should be controlled to attain the high mode conversion efficiency from the O/X-mode wave to the B-mode wave, depending the plasma current and density. A phased-array antenna system, which enabled us to control the launching angle and polarization, was proposed and has been developed for the EBWH/CD experiments in the QUEST. The antenna excited the electromagnetic O-mode wave in the oblique injection, not taking direct coupling into the electrostatic B-wave in front of the antenna like a grill antenna for the lower hybrid current drive (LHCD) experiments as proposed previously [4].

In order to study wave propagation and absorption of the B-wave, the wave trajectory has been calculated with some ray tracing codes, for instance in [5]. The ray trajectory of the incident wave was calculated with the TASK/WR ray-tracing code [6] on the QUEST in a case of an optimum O-mode incident condition [7]. The local wave electric fields along the propagation were evaluated in the ray trace calculation, and used for the Fokker-Planck (FP) analysis using the TASK/FP code [6]. The driven-current profile was estimated with the FP analysis in the optimum incident condition [7]. The obtained dimensionless current drive efficiency [8] was comparable to the W-7AS stellarator's experimental result [9]. The O-X mode conversion depended on the incident refractive index  $N_{//}$  in parallel to the magnetic field. In the non-optimum incident case, the tunneling effect through an evanescent layer should be properly treated, taking the mode conversion efficiency into consideration. The propagation and absorption of the multiple rays after the mode conversions were analyzed using the modified TASK/WR code here.

This paper is organized as follows. The experimental scenario using the O-X-B mode conversion is described in Section 2. Section 3 explains a concept of the proposed phased-array antenna system. The heat load and thermal stress in the CW operation were analyzed, and the radiation fields from the antenna were tested at a low power level. These design works and the performance tests of the antenna system are described in Sections 4. Section 5 describes the development of fast phase shifters to adjust the launching polarization and angle in feedback control. The multiple-ray tracing is introduced to evaluate the power deposition profile, concerning the antenna setup problem. The initial results of the plasma startup and sustainment in long-pulse discharges are shown in Section 6, and the conclusion is finally given in Section 7.

## 1. Experimental Scenario using O-X-B mode conversion

The QUEST project has focused on study how to sustain plasma current by the EBWH/CD for the PWI study in steady-state operation. In the QUEST, the major and plasma radii were 0.68 m and 0.36 m, respectively. The maximum toroidal field was 0.25 T in the steady state operation. It was planned to sustain the rather low plasma current of 20kA in the lower density region, but in the steady state, as a first target of the QUEST project. In these experiments, the plasma current will start up by only the RF-wave injection without an induced electric field [10-13]. In rather low-density gradient case, the O-X-B mode conversion scenario was suitable to take the high conversion efficiency into the B-mode wave [14]. The incident O-mode wave obliquely launched from the low field/density side was converted to the X-mode wave. The optimum parallel refractive index  $N_{//}^{\text{opt}}$  for the oblique injection at the O-cutoff layer was given by

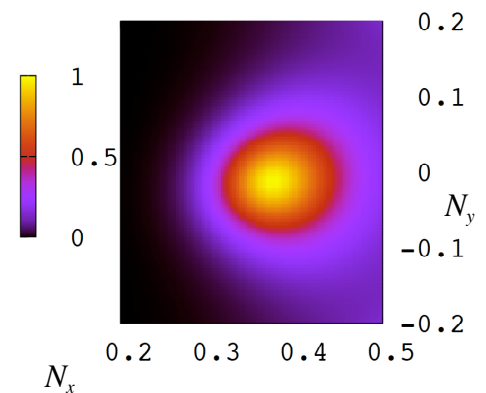
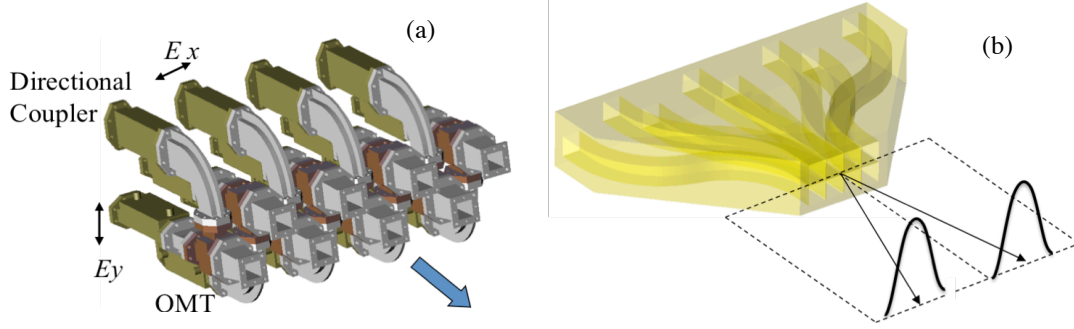


Fig.1: Contour plot of mode conversion efficiency as functions of horizontal and vertical refractive indexes,  $N_x$  and  $N_y$ .



*Figs.2: Conceptual design of phase-array antenna system for EBWH/CD experiments in the QUEST. (a): Orthomode transducer part to control launching polarization state. (b): Phased-array antenna part to control launching angle for the magnetic field. The 8 [4x2] squared waveguide ports are prepared to take the polarized phased array.*

$N_{\parallel}^{\text{opt}} = \sqrt{Y/1+Y}$ , where  $Y$  was a ratio of the electron cyclotron frequency  $\omega_{ce}$  to the wave frequency  $\omega$ . The incident O-mode wave was converted into an X-mode wave at the O-cutoff, and propagated as the X-mode wave. The X-mode wave reached the upper hybrid resonance, and converted to the B-mode wave. The B-mode wave was fully absorbed due to the Doppler shifted resonance. The contour plot of the calculated mode conversion efficiency is shown in Fig.1 as functions of initial launching horizontal and vertical refractive indexes,  $N_x$  and  $N_y$  [15]. The effective refractive-index window with moderate conversion efficiency was within the range of +/- 0.1 for the optimum indexes. In the calculation, the plasma current and the magnetic field were assumed to be 20 kA and 0.25 T. Parabolic density and temperature profiles were taken here with the central density and temperature of  $2 \times 10^{18} \text{ m}^{-3}$  and 100 eV. The advanced antenna system was required to inject the oblique O-mode beam in the mode conversion experiments.

### 3. Conceptual Design of Antenna System

The 8.2 GHz system was prepared for the LHCD experiments in the previous TRIAM-1M tokamak at Kyushu University. This 8.2 GHz system has been used for the EBWH/CD experiments in the QUEST. In the system, a maximum power of 200 kW generated by 8 klystrons was transmitted using 16 rectangular fundamental waveguide (WR-137) lines in the CW operation. An orthomode transducer (OMT) was designed to control launching polarization state in the proposed antenna system. In order to excite a pure O-mode in the oblique injection, the elliptical polarization control was required. Figure 2(a) shows the OMT part of the phased-array antenna system. The directional couplers measured the intensity and phase of the transmitted wave to take the polarized phase array. The two orthogonal electric field components were mixed to excite arbitrary elliptical polarization states with the intensity and phase control between of them. The orthomode transducer was designed to be optimum for the open-end operation. The voltage standing wave ratio (VSWR) was evaluated using a 3D full-wave electromagnetic field simulator, HFSS code. The VSWR at the open-end operation was less than 1.1 at the operating frequency of 8.2 GHz. The 8 OMT square waveguide outputs were led into the phased-array antenna to control the launching angle as shown in Fig. 2(b). The output aperture of the antenna was composed of the 8 [4x2] squared waveguide phased-array ports.

### 4. Development of CW phased-array antenna for EBWH/CD experiments in QUEST

The antenna structure has been considered to take a good oblique directivity of the beam for the O-X-B mode conversion experiments. The radiation field property was strongly

depended on a side and wall thickness of the squared waveguide ports. The wall thickness should be reduced to take an applicable radiation field without large side-lobes. The thin waveguide wall caused poor thermal conductivity there. In the first antenna design with an enforced cooling structure, the thermal stress due to the increment of the temperature in the CW operation was beyond the yield stress of an oxygen-free copper of the antenna material [16]. The antenna structure with the enforced water-cooling was modified to avoid a permanent set due to the thermal stress. The brazing fabrication technique was also revised into an electron beam welding technique to cut anneal processes causing reduction of yield stress. The heat load and thermal stress have been analyzed with the HFSS and ANSYS codes. Figure 3 shows the increased temperature distribution of a finally designed antenna in the CW 200 kW operation. The maximum temperature was 67 degree C, and the thermal stress was analyzed to be moderate.

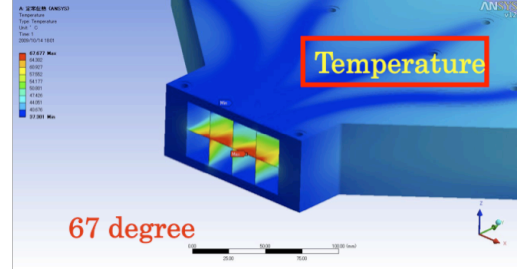
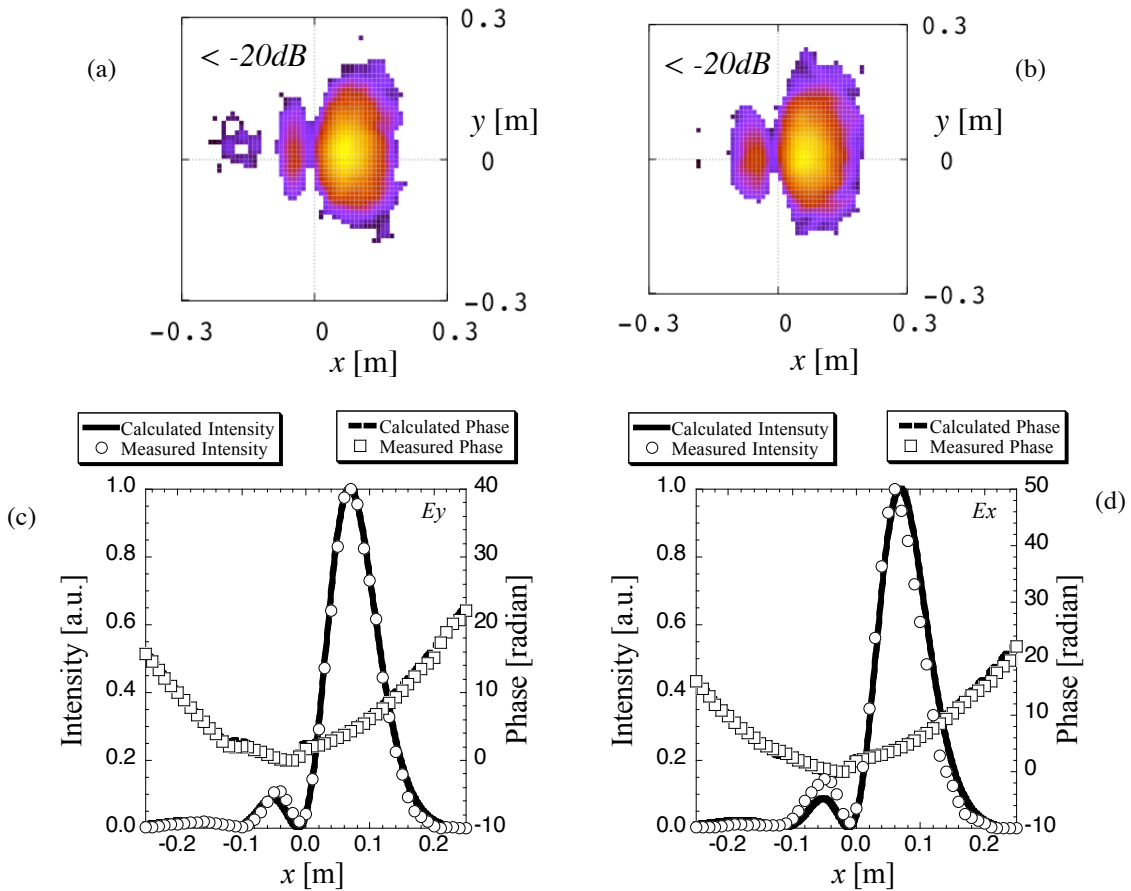


Fig.3: Increased temperature distribution of a finally designed phased-array antenna in the CW 200 kW operation. Maximum temperature is 67 degree C, and the resulted thermal stress is analyzed to be moderate.

The [4x2] phased-array antenna was fabricated for the EBWH/CD experiments in the QUEST along the design works, and was tested in the low power test facilities at Kyushu



Figs.4: Radiation fields in vertical  $E_y$  and horizontal  $E_x$  components radiated from the CW phased-array antenna, Logarithmic contour-plots of the measured  $E_y$  and  $E_x$  components are shown in Figs 4(a) and 4(b). Measured intensity and phase  $x$  profiles of the  $E_y$  and  $E_x$  components are shown in Figs.4(c) and 4(d), as well as the profiles calculated with a developed Kirchhoff integral code.

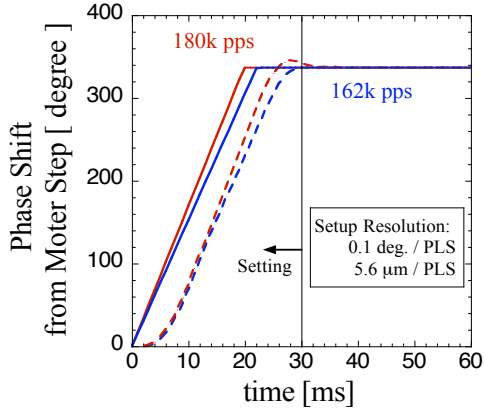


Fig.5: Fast plunger position control of a 3dB hybrid phase shifter. Solid and dashed curves show controlling and resulted positions in the fast scanning, respectively.

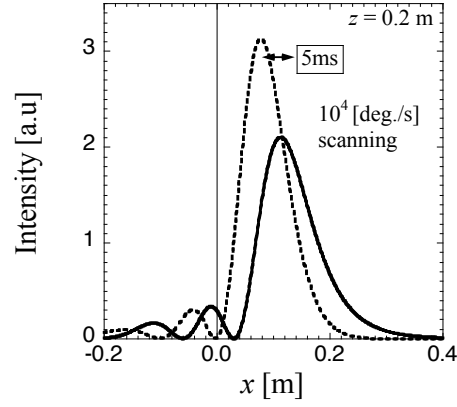


Fig.6: Fast launching-angle scanning using developed phase shifters within 5 ms. The scanning speed is  $10^4$  degree/s as shown in Fig.5.

University. Figures 4(a) and 4(b) show contour plots of the intensity patterns radiated from the developed CW antenna system in vertical  $E_y$  and horizontal  $E_x$  field components. There were focused main beams in the steered horizontal  $x$  direction with no large side-lobes in both two field components. The fields were measured at a propagating  $z$  position of 0.2 m. Figures 4(c) and 4(d) show the measured intensity and phase profiles in the  $x$  direction as well as the calculated profiles with a developed Kirchhoff integral code. The Kirchhoff integral was expressed as

$$E_{x,y}(x,y,z) = \frac{ik}{2\pi z} \int_{-a/2}^{a/2} \int_{-a/2}^{a/2} dx' dy' E_{x,y}(x',y') [\exp(-ikr)/r],$$

$$r = \sqrt{(x-x')^2 + (y-y')^2 + z^2},$$

where the coordinates of  $(x', y')$  and  $(x, y)$  were at the antenna aperture position ( $z = 0$ ) and at the radiated  $z$  position. Here,  $a$  was a side of the square-waveguide, respectively. The measured intensity and phase profiles were in excellent agreements with the calculated profiles in both the two electric field components as shown in the figures. The developed phased-array antenna worked correctly along the design to excite a pure O-mode wave in the oblique injection.

## 5. Feedback Control of Phased Array

The optimum incident condition depended on the plasma current and density profile/gradient. The incident polarization and angle should follow to their time evolutions to attain high mode conversion efficiency into the B-wave. The fast 3dB hybrid phase shifter has been developed and installed to the CW transmission lines. The plunger position of the phase shifter was scanned to control the transmitted wave phase. The attained scanning speed of the phase by the plunger position control was  $10^4$  degree/s as shown in Fig.5. The polarization can be controlled within 9 ms from a linear to a circular polarization state. Figure 6 shows the fast beam steering within 5 ms. The FPGA control system, including the reflectometry diagnostics [17] to measure the density profile, is preparing to control 16 phase shifters in parallel in feedback loops to obtain the optimum incident polarization and angle.

## 6. Multiple Ray Analysis in O-X-B mode conversion

In the non-optimum incident case of the O-X-B mode conversion, the tunneling effect through the evanescent layer should be properly treated. The ray trajectory was analyzed, taking the tunneling effect into consideration in a single ray analysis in a non-optimum case.

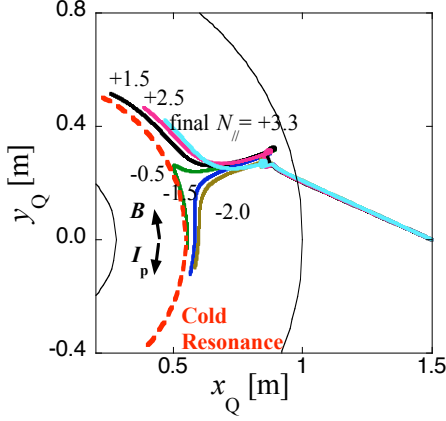


Fig.7: Ray trajectories with  $N_{||}$  varying along propagations in the multiple-ray analysis. The  $N_{||}$  signs are changed along the propagations in some rays. The final  $N_{||}$  are remarked in the figure.

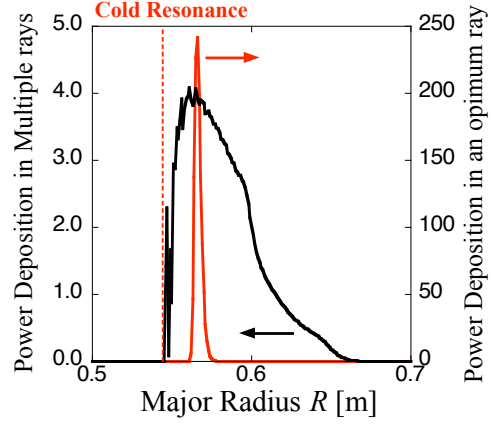


Fig.8: Broad and peaked power deposition profiles in the multiple ray analysis with various  $N_{||}$  evolutions and in an optimum case, respectively.

The ray position after the tunneling was searched in the high-density side beyond the cutoff [18]. This approach was implemented into the TASK/WR code for the multiple-ray tracing. Figure 7 shows calculated ray trajectories at the O-X-B mode conversion in a toroidal cross-section until the B-wave was fully absorbed due to Doppler-shifted resonances with  $N_{||}$  varying along the propagations. Here, a coordinate  $(x_Q, y_Q, z_Q)$  system with an origin at the QUEST device was taken in the multiple ray analysis. The  $y_Q$  and  $z_Q$  coordinates were expressed in toroidal and poloidal directions at the launching antenna position of  $z_Q=0$ . The initial poloidal refractive indexes  $Nz_Q$  were scanned with a fixed initial toroidal index  $Ny_Q$ , respectively. The calculated conditions were identical to those used in Fig.1. Figure 8 shows a broad power deposition profile in the multiple ray analysis with the various  $N_{||}$  evolutions, as well as a peaked deposition profile in an optimum case. The mode conversion efficiencies were taken into account for each ray in the multiple-ray tracing. The changes of the  $N_{||}$  sign from plus [+] to minus [-] were observed along the propagation in some rays, which was not desired for the current drive experiments. It was pointed out that the wave directionality could be determined by launching the waves above or below the mid-plane of the torus and was related to a geometric effect on the poloidal magnetic field [19]. The antenna setup position was considered along the multiple ray analysis. The fraction of power absorption  $P_{abs}$  for each ray was evaluated as

$$P_{abs} = -2 \text{sgn}(\mathbf{I}_p \cdot \mathbf{B}) \text{sgn}(N_{||}) \frac{\partial \text{Im}D}{\partial s}$$

using the wave dispersion function  $D$ , taking signs of a scalar product  $(\mathbf{I}_p \cdot \mathbf{B})$  with current and magnetic field vectors and  $N_{||}$ . The minus [-] power fraction component was acceptable for the current drive experiments. Figure 9 shows radial profiles  $\Delta P_{abs}$  of the differences between [ $\pm$ ]  $P_{abs}$  components in the multiple rays for the antenna positions of  $z_Q = 0$  and  $-0.08$  m. The minus [-] absorbed fraction component was significantly large at the antenna setting of  $z_Q = -0.08$  m. The setting position was limited geometrically by size of a vacuum vessel installing the

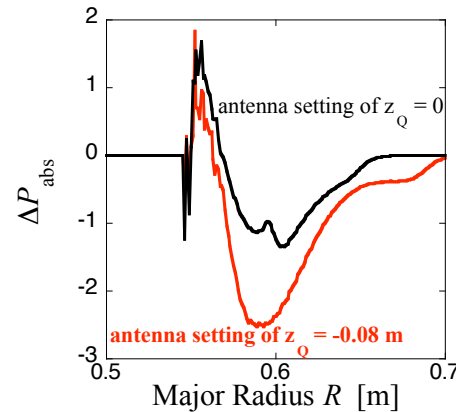
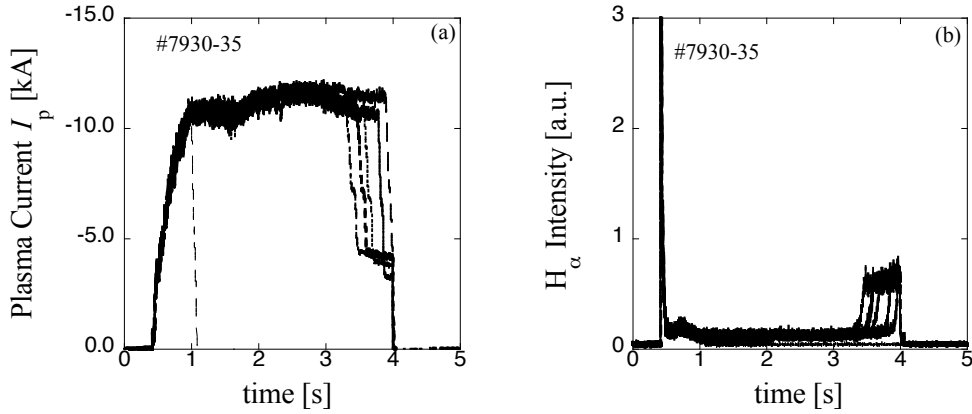


Fig.9: Radial profiles  $\Delta P_{abs}$  of differences between [ $\pm$ ]  $P_{abs}$  components for the antenna settings at the mid-plane of  $z_Q = 0$  and below the mid-plane of  $z_Q = -0.08$  m.



Figs.10: Typical time evolutions of (a): plasma current and (b):  $H\alpha$  intensity in non-inductive current drive experiments on the QUEST in the last experimental campaign. The discharges are terminated with enhanced recycling caused by increments of the  $H\alpha$  intensity.

antenna system. The desired antenna positions above or below the mid-plane remarkably depended on the plasma current and toroidal magnetic field directions. The antenna was installed below the mid-plane at this time, and the RF-plasma startup and sustainment experiments in long-pulse discharges have been begun without an induced electric field in the QUEST.

## 6. Initial Results of RF Plasma Start up and Sustainment in Long-pulse Discharges

The non-inductive plasma current drive experiments have been begun using the developed phased-array antenna system in the last experimental campaign. Figures 10 show typical time evolutions of the plasma current  $I_p$  and the  $H\alpha$  intensity in the RF plasma startup experiments. The vertical magnetic field  $B_z$  with two pairs of the poloidal magnetic coils (PFC1-7/2-6) was ramped up to about 3 mT. The toroidal magnetic field was 0.133 T, and the injected power was 35 kW. The hard X-ray intensity from current-carrying forward electrons accelerated by the RF injection was increased in the energy range of 10~30 keV, following the  $I_p$  evolution. Figure 11 shows the  $I_p$  evolution as a function of the ramped-up vertical field  $B_z$  at the major radius  $R = 0.68$  m. The plasma current was ramped up along the  $B_z$  evolution, but the discharge was terminated due to the recycling enhancement or the increment of the  $H\alpha$  intensity. Figure 12 shows reconstructed magnetic flux surfaces of the 12 kA discharge using

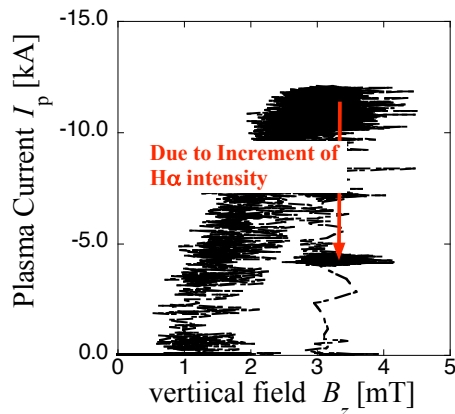


Fig.11: Plasma current ramped up, following  $B_z$  evolution, in the 12 kA discharge.

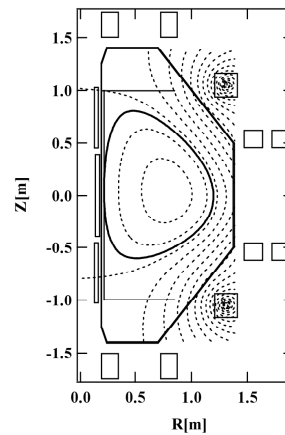


Fig.12: Reconstructed flux surfaces in the 12 kA discharge. The aspect ratio is 1.5.

the parabolic current fitting method [20]. The ST plasma with a low aspect ratio of 1.5 was attained in these experiments. The maximum current in the RF startup experiment was 15 kA at the 85 kW injection using one more 8.2 GHz system together with. The long-pulse discharge of 10 kA was attained for 40 sec at a constant  $B_z$  with the 30 kW injection. The asymmetric confinement structure of high energetic electrons on the parallel velocity in a velocity space was one of candidates to explain the generated current. The density was lower than the O-mode cutoff density at the low magnetic field in these experiments, because of difficulty to overcome recycling enhancement. The O-X-B mode conversion experiments will be conducted using the developed phased-array antenna in over-dense plasmas.

## 7. Conclusion

The phased-array antenna system was proposed and has been developed to conduct the O-X-B mode conversion experiments in the QUEST. The launching polarization and angle were controlled with the orthomode transducer and the phased-array antenna parts designed for the CW operation. The heat load and the thermal stress at the antenna were analyzed to be moderate in the CW 200 kW operation. The measured radiation fields were explained well with the developed Kirchhoff integral code. The multiple ray trajectories were analyzed, taking the tunneling effect at the mode conversion into account. The plasma current  $I_p < \sim 15$  kA with the aspect ratio of 1.5 was started up and sustained by only RF injection, but terminated by enhancement of the recycling. The long pulse discharge of  $I_p \sim 10$  kA was attained for 40 s with the 30 kW injection. The O-X-B mode conversion experiments will be conducted using the phased-array antenna in over-dense plasmas, also in the feedback control using the fast scanning [ $\sim 10^4$  degree/s] phase shifters.

## Acknowledgments

This work was partially supported by a Grant-in-aid for Scientific Research (21360452). This work was performed with the support and under the auspices of the NIFS Collaboration Research Programs (NIFS09KUTR036, NIFS09KUTR046, NIFS10KUTR054).

## References

- [1] Hanada, K. *et al.*, Proc. of the 22<sup>nd</sup> IAEA Fusion Energy Conference (2008), FT/P3-25.
- [2] Laqua, H.P. *et al.*, Phys. Rev. Lett. **78** (1997) 3467.
- [3] Laqua, H.P. *et al.*, Plasma Phys. Control. Fusion **49** (2007) R1, and references therein.
- [4] Pinsker, R.I. *et al.*, Plasma Phys. Control. Fusion **47** (2005) 335.
- [5] Maekawa, T. *et al.*, J. of the Phy. Soc. of Japan **48** (1980) 247.
- [6] Fukuyama, A., Fusion Eng. and Design, **53** (2001) 71.
- [7] Idei, H. *et al.*, J. of Plasma Fusion Res. Series, **8** (2009) 1104.
- [8] Luce, T. C. *et al.*, Phys. Rev. Lett. **83**, (1999) 4550..
- [9] Laqua, H.P. *et al.*, P Phys. Rev. Lett. **90** (2003) 75003.
- [10] Maekawa, T. *et al.*, Nucl. Fusion **45** (2005) 1439.
- [11] Yoshinaga, T. *et al.* Proc. of the 22<sup>nd</sup> IAEA Fusion Energy Conference (2008), EX/P6-9.
- [12] Ejiri, A. *et al.*, Nucl. Fusion **49** (2009) 0655010.
- [13] Shevchenko, V.F. *et al.*, Nucl. Fusion **50** (2010) 022004
- [14] Igami, H. *et al.*, Plasma Phys. Control. Fusion **48** (2006) 573.
- [15] Mjølhus, E. J. Plasma Phys. **31** (1984) 7.
- [16] Idei, H. *et al.*, Proc. of the 34<sup>th</sup> Int. Conf. on Inf. and Millimetre Waves, (2009) R2D04.
- [17] Idei, H. *et al.*, J. of Plasma Fusion Res. Series, **9** (2010) 112.
- [18] Igami, H. *et al.*, Plasma Science and Technology. **11** (2009) 430.
- [19] Forest, C.B. *et al.*, Phys. Plasmas, **7** (2000) 1352.
- [20] Yoshinaga, T. *et al.*, Nucl. Fusion **47** (2007) 210.